Received: 2 February 2022 | Revised: 22 August 2022 | Accepted: 23 August 2022

DOI: 10.1002/hbm.26067

RESEARCH ARTICLE

WILEY

Attentional M100 gain modulation localizes to auditory sensory cortex and is deficient in first-episode psychosis

Mark T. Curtis | Xi Ren | Brian A. Coffman | Dean F. Salisbury

Clinical Neurophysiology Research Laboratory, Western Psychiatric Hospital, Department of Psychiatry, University of Pittsburgh School of Medicine, Pittsburgh, Pennsylvania, USA

Correspondence
Dean F. Salisbury, CNRL, 3501 Forbes Ave, Suite 420, Pittsburgh, PA 15213, USA.
Email: salisburyd@upmc.edu

Funding information
National Institute of Mental Health, Grant/Award Numbers: F31 MH119718, R01 MH108568, RO1 MH113533

Abstract

Selective attention is impaired in first-episode psychosis (FEP). Selective attention effects can be detected during auditory tasks as increased sensory activity. We previously reported electroencephalography scalp-measured N100 enhancement is reduced in FEP. Here, we localized magnetoencephalography (MEG) M100 source activity within the auditory cortex, making novel use of the Human Connectome Project multimodal parcellation (HCP-MMP) to identify precise auditory cortical areas involved in attention modulation and its impairment in FEP. MEG was recorded from 27 FEP and 31 matched healthy controls (HC) while individuals either ignored frequent standard and rare oddball tones while watching a silent movie or attended tones by pressing a button to oddballs. Because M100 arises mainly in the auditory cortices, MEG activity during the M100 interval was projected to the auditory sensory cortices defined by the HCP-MMP (A1, lateral belt, and parabelt parcels). FEP had less auditory sensory cortex M100 activity in both conditions. In addition, there was a significant interaction between group and attention. HC enhanced source activity with attention, but FEP did not. These results demonstrate deficits in both sensory processing and attentional modulation of the M100 in FEP. Novel use of the HCP-MMP revealed the precise cortical areas underlying attention modulation of auditory sensory activity in healthy individuals and impairments in FEP. The sensory reduction and attention modulation impairment indicate local and systems-level pathophysiology proximal to disease onset that may be critical for etiology. Further, M100 and N100 enhancement may serve as outcome variables for targeted intervention to improve attention in early psychosis.

KEYWORDS
auditory evoked potential, first episode, N100, psychosis, selective attention

1 | INTRODUCTION

Cognitive deficits are a core feature of psychotic disorders that are present before psychosis, endure throughout the disorder, and are

The NIH played no role in the collection or analysis of data or in the preparation of this manuscript.

associated with long-term functional outcome (Caspi et al., 2003; Fett et al., 2011). A fundamental cognitive deficit that predates the onset of psychosis is the impairment of selective attention (Cornblatt et al., 2003; Kraepelin, 1889). Selective attention, the focusing on one percept among other competing stimuli, is a cognitive process essential for facilitating task performance. Cross-modal attention, for example, attending sounds while ignoring a movie or vice versa, represent a type of selective attention well explored in cognitive psychology (Parasuraman, 1985). In humans, this aspect of selective attention can be measured in the auditory system with high temporal resolution using electroencephalography (EEG) and magnetoencephalography (MEG). Late sensory processing of sounds is measured by the event-related negativity present ~100 ms poststimulus (N100) for EEG and its MEG counterpart (M100). While the N100/M100 automatically occurs in response to a sound, when healthy individuals pay attention to a sound, N100/M100 amplitudes increase relative to ignore or divided attention conditions (Hillyard et al., 1973; Neelon et al., 2006; Woldorff et al., 1993). Individuals with schizophrenia have an impaired passive N100 response and an impaired ability to enhance the N100 with attention (Foxe et al., 2011; O'Donnell et al., 1994; Rosburg et al., 2008), demonstrating that the N100 is sensitive to both bottom-up sensory perceptual deficits and top-down executive modulation with attention in psychosis. These impairments are present as early as the first episode of psychosis (FEP). Individuals at their FEP have a reduced N100, though it is unclear if this was primarily due to a sensory or executive deficit (Foxe et al., 2011; Salisbury et al., 2010). Comparing attend and ignore conditions, we recently demonstrated that the attentional gain modulation of N100 is deficient in FEP (Ren et al., 2021). Thus, N100 enhancement is an objective measure of selective attention deficits very early in psychosis. While the majority of sensory N100/M100 arises in auditory sensory cortex, the dysfunction in N100 enhancement indexes a distributed cortical circuit involving the interaction of frontal executive and temporal auditory areas and presents a neurobiological system amenable for targeted intervention. However, it is unknown which auditory cortical areas contribute to this deficit in sensory gain, critical for both understanding the local cortical circuit deficits and for development of targeted interventions, whether employing pharmacologic or noninvasive brain stimulation (NIBS) techniques.

The general cortical network underlying selective attention involves the prefrontal cortex, through connections with posterior parietal cortex, modulating activity in sensory cortices (Petersen & Posner, 2012; Tobyne et al., 2017). In monkey visual cortex, attention enhances neuronal responses in striate (V1), pre-striate (V2), and extra-striate cortex (V4) (Luck et al., 1997; McAdams & Reid, 2005; Spitzer et al., 1988). In the auditory domain, work in ferrets suggests prefrontal cortex modulates activity in auditory cortex at multiple hierarchical levels, with primary auditory cortex and surrounding auditory belt areas playing an important role in auditory selective attention (Elgueda et al., 2019; Fritz et al., 2003). Similar enhancement with attention in auditory cortex is seen in humans, with multimodal imaging demonstrating that selective attention enhances activity in both primary and nonprimary auditory cortex (Ahveninen et al., 2006; Petkov et al., 2004). Despite this evidence, human research has been limited in determining cortical areas differentially involved in specific processes by being restricted to identifying only relatively large, anatomically defined regions of interest in auditory cortex (e.g., Heschl's gyrus), with a lack of specificity between primary and other nonprimary auditory cortex areas that is necessary for animal models (e.g., primary auditory cortex vs. auditory belt areas). The Human Connectome Project's multimodal parcellation (HCP-MMP) delineates primary auditory cortex (A1) and auditory belt areas in humans that cannot be defined by previous in vivo methods. While previous parcellation methods typically rely on one modality alone to define cortical regions, the HCP-MMP was developed by utilizing myelination, resting state connectivity, and task-based connectivity information, which allows for the definition of these functional areas. Importantly, it also has clear correspondence to human postmortem and monkey tracing studies (Glasser et al., 2016; Sweet et al., 2005), and thus can identify valid functional distributed systems. In addition, the collection of multimodal data (e.g., structural MRI and resting-state functional MRI) and implementation of the HCP processing pipelines allows for myelination and resting-state connectivity information to drive alignment between individuals with a multimodal surface matching (MSM) registration technique. Traditionally, alignment of cortical surfaces was limited to one modality, such as curvature, but the flexible MSM framework allows for the addition of other useful information such as resting state connectivity to help drive alignment, ultimately improving the cortical surface alignment between individuals (Coalson et al., 2018; Glasser et al., 2016; Robinson et al., 2014). This improved alignment decreases variability of areal definition between individuals and increases confidence of correct correspondence of areas between individuals.

We source-resolved the M100 to identify where cross-modal selective attention increased M100 gain, and where auditory sensory and attention-related deficits arise in FEP, which have not previously been directly investigated. While fMRI provides high spatial resolution, the measure of neural activity is indirect and less sensitive to changes at high temporal resolution. EEG and MEG provide an advantage over previous studies examining attention modulation, as neural activity can be measured directly on the scale of milliseconds, necessary for the measurement sensory processes such as the N100/M100, and the rapid modulation of these processes with attention. Compared to EEG, MEG provides an improved source solution for determining cortical generators inside the head from sensors outside the head because magnetic fields are unaffected by the skull and skin, while keeping the high temporal resolution needed to detect rapid neural activity. Understanding the precise cortical areas underlying this impaired ability to modulate the N100/M100 with selective attention in the early disease course can provide insight to the etiology of the disorder and identify potential targets for therapeutic interventions and anatomic circuit locations for translation to animal models.

In this study, we recorded MEG data during a cross-modal auditory attention task in 27 individuals within 2 months of their first clinical contact for their FEP and 31 matched healthy controls (HC).

Submillimeter-resolution MRI data were also collected to create individual head models for source localization of the auditory M100 and its enhancement by attention. Multimodal MRI data (structural MRI and resting-state fMRI) were collected for the novel utilization of the HCP pipelines and HCP-MMP to precisely parcellate auditory cortex provided the ability to determine the specific auditory cortex areas involved in M100 attention modulation and which areas underlie auditory sensory and attention deficits in FEP.

2 | METHODS AND MATERIALS

2.1 | Participants

All participants were recruited from Western Psychiatric Hospital (WPH) inpatient and outpatient services. Participants included 27 FEP individuals within their FEP with less than 2 months of lifetime antipsychotic medication exposure, and 31 HC. No participant had a history of concussion or head injury with sequelae, history of alcohol or drug addiction or detox in the last 5 years, or neurological comorbidity. Groups were matched for age, gender, parental social economic status, and premorbid IQ, measured by the vocabulary component of the Wechsler Abbreviated Scale of Intelligence (WASI) (Table 1). The WASI vocabulary subtest is a measure of semantic knowledge, an IQ measure relatively resistant to psychosis, neurodegeneration, and deterioration over time (Bilder et al., 1988; de Oliveira et al., 2014; Eberhard et al., 2003; Heaton et al., 2001; Hoff et al., 1999; Kremen et al., 1995; Mohn-Haugen et al., 2022). All participants had healthy hearing confirmed with audiometry. All participants provided informed consent and were paid for participation. The work described was carried out in accordance with The Code of Ethics of the World Medical Association (Declaration of Helsinki) for experiments involving humans.

All tests were conducted by an expert clinical diagnostician. Socioeconomic status for all participants and their parents was measured with the four-factor Hollingshead Scale. FEP participants' diagnoses were based on the Structured Clinical Interview for DSM-IV (First et al., 1997). Provisional research diagnoses were initially at baseline, and then confirmed 5–7 months later. Symptoms were rated using the Positive and Negative Syndrome Scale (PANSS) (Table 1) (Kay et al., 1987). The PANSS is a 30-item assessment that measures positive symptoms, negative symptoms, and general psychopathology. Current cognitive ability was assessed with the MATRICS Consensus Cognitive Battery (MCCB) (Nuechterlein et al., 2008) for all participants (HC and FEP). MCCB items were selected to capture the state-dependent effect of psychosis on cognition, whereas WASI vocabulary provides a more stable estimate of premorbid intellect. The MCCB is a standardized cognitive battery that provides a reliable and valid evaluation of functioning in the following cognitive domains: speed of processing, attention/vigilance, working memory, visual learning, reasoning and problem solving, and social cognition. Despite estimated premorbid WASI IQ, the MCCB composite score was significantly reduced in this FEP sample (see Table 1) as expected due to the effects of acute psychosis (Kern et al., 2011; Nuechterlein et al., 2008).

TABLE 1 Demographic, neuropsychological, and clinical information. FEP and HC groups were matched for age, gender, PSES, and WASI Vocab T-score (Mean (SD))

	FEP	HC	t/X^2	p
Age	23.4 (4.5)	24.9 (5.7)	−1.12	.27
Gender (M/F)	17/10	22/9	0.42	.52
SES	29.8 (13.9)	41.8 (13.1)	−3.39	<.01
Parental SES	43.3 (13.4)	48.5 (10.9)	−1.64	.11
WASI Vocab T-score	49.2 (9.6)	52.7 (6.2)	−1.67	.11
MCCB-total	30.8 (14.6)	50.7 (7.2)	−6.71	<.01
PANSS total	76.7 (19.8)			
PANSS positive	20.0 (6.5)			
PANSS negative	17.9 (6.0)			
PANSS general	38.9 (9.8)			
SAPS global	6.2 (3.7)			
SANS global	10.1 (4.1)			
Medication	242.3 (139.5)			

Note: Medication, chlorpromazine equivalents.
Abbreviations: FEP, first-episode psychosis; MCCB, MATRICS Consensus Cognitive Battery composite scaled t score; PANSS, Positive and Negative Syndrome Scale; SANS, Scale for the Assessment of Negative Symptoms; SAPS, Scale for the Assessment of Positive Symptoms; SES, socioeconomic status; WASI, Wechsler Abbreviated Scale of Intelligence.

Of the 27 FEP participants, 22 received diagnoses on the schizophrenia spectrum (FESz). Seventeen received diagnoses of Schizophrenia (paranoid: $n = 7$; undifferentiated: $n = 10$), one of schizoaffective disorder (bipolar subtype), two of schizophreniform (definite), and two of psychotic disorder NOS. Five individuals received diagnoses of affective disorders: four of bipolar I disorder and one major depressive disorder. While many of the FEP participants were medicated (21/27, 78%), chlorpromazine equivalent dose did not correlate with source values from either condition or region (p values >.1). In addition, there was no significant group difference between medicated and unmedicated individuals ($F(1,25) = 0.895$, $p = .353$, $\eta_p^2 = .035$), and no significant interaction between medication group and attention modulation ($F(1,25) = 0.289$, $p = .596$, $\eta_p^2 = .011$). Details of the medication types are provided in the supplementary materials (Supplementary Table S1). Medication will not be addressed further.

2.2 | Task

A classic oddball task with a frequent tone and a rare tone was presented in two conditions to each participant. Stimuli consisted of a standard tone (1 kHz, 50 ms duration, 10 ms rise/fall) and a deviant tone (1.2 kHz, 50 ms duration, 10 ms rise/fall) presented with a stimulus onset asynchrony of 1050–1550 ms. A total of 400 tones were

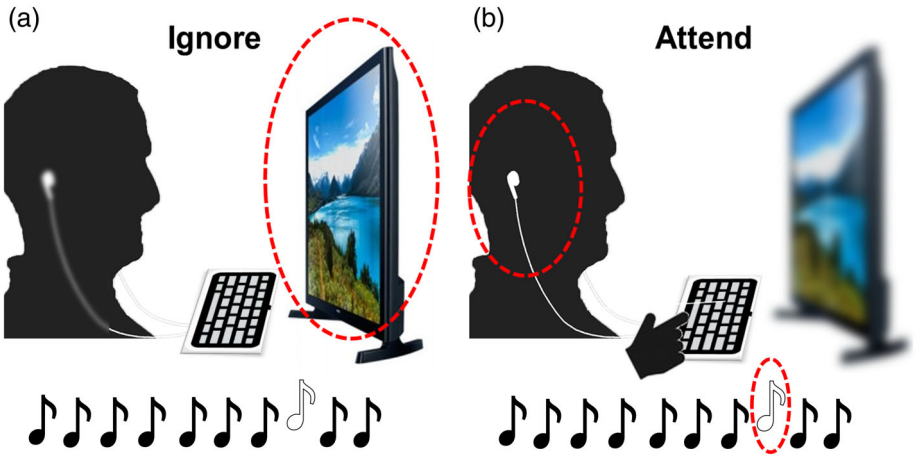

FIGURE 1 Auditory attention task. (a) In the ignore condition, individuals ignored the tones and attended to a silent film. (b) In the attend condition, individuals ignored the silent film and attended to the tones and pressed a button when the tone changed in pitch

presented, including 340 standard tones (85%) and 60 deviant tones (15%). In one condition, participants were asked to ignore the tones and attend to a silent video. In the second condition, participants were asked to pay attention to the tones and press a button to every deviant tone (Figure 1). Blocks were counterbalanced. Only M100 responses to standard tones (not deviant oddballs) were analyzed.

2.3 | MEG data acquisition and processing

MEG data were recorded in a magnetically shielded room with a 306-channel whole-head system (Elekta Neuromag), consisting of 128 triplets (1 magnetometer and 2 planar gradiometers). Data were recorded using a sampling rate of 1000 Hz (online band-pass filter = 0.1–330 Hz). Eye blinks and movements were recorded with bipolar leads placed above and below the left eye (VEOG) and lateral to the outer canthi of both eyes (HEOG). Cardiac activity was recorded with bipolar ECG leads. A 3D-digitizer (ISOTRAK; Polhemus, Inc., Colchester, VT) was used to continuously record the location of four head position indicator coils placed on the scalp of each participant relative to their nasion and preauricular points. Further, additional points on the head and face were recorded to aid in the registration to MRI data. Neuromag MaxFilter software (http://imaging.mrc-cbu.cam.ac.uk/meg/Maxfilter_V2.2) was used to correct for head motion during the scan. Temporal signal space separation was used to remove electromagnetic noise originating from outside the MEG helmet (Uusitalo & Ilmoniemi, 1997). The EEGLAB Toolbox (Delorme & Makeig, 2004) in MATLAB was used to remove channels and segments of data with excessive noise via visual inspection. A high-pass filter (0.5 Hz; 12 dB/oct) was applied to the data, and an adaptive mixture independent component analysis was performed to remove eye-blink and ECG components.

Offline processing of the MEG was performed with Brainstorm (Tadel et al., 2011), which is documented and freely available for download online under the GNU general public license (http://neuroimage.usc.edu/brainstorm). A low-pass (20 Hz) filter was applied to the data to remove muscle and other high-frequency artifacts. Trials were then segmented from 100 ms before to 1000 ms after stimulus onset. The average baseline voltage was subtracted, and trials that exceeded were ±5 pT were rejected. The remaining trials were averaged.

In Brainstorm, MEG sensor data were registered to each participant's structural MRI in two steps. Initially, the registration was based on three fiducial points (nasion, left ear, and right ear) that are marked on the individual's MRI and on the participant before the MEG acquisition. The points measured before acquisition were aligned with those marked on the MRI within Brainstorm. The second step refined the registration with the digitized points collected at acquisition and the MRI head surface imported from FreeSurfer (see MRI methods below). Each registration was manually inspected for accuracy. Possible sources were constrained to the individual's cortical surface. The forward solution was modeled as overlapping spheres, and a noise covariance matrix was calculated from the baseline window of all trials. Cortical source activity was estimated using minimum norm estimation with a dipole constraint of 0.4 and depth weighting applied. Current density values were normalized with the use of dynamic statistical parametric maps (dSPM) based on the variance in the prestimulus baseline. Auditory cortex regions of interest were bilateral A1, LBelt, and PBelt, defined by the HCP-MMP. Activity within these ROIs was measured over the 80- to 140-ms poststimulus time window, which was consistent with previous measurement methods and was chosen to capture the M100 peak and attention effects without overlapping the subsequent component (Figure 2a).

2.4 | MRI data acquisition and processing

Submillimeter resolution MRI data were acquired on a Siemens 3 T MAGNETOM Prisma scanner using a 32-channel phase array head coil. Sagittal T1-weighted anatomical MR images were obtained with a 3D MPRAGE sequence (TR/TE/TI = 2400/2.22/1000 ms, flip angle = 7°, field of view [FOV] = 256 × 240 mm, 0.8 mm isotropic voxel size, 208 slices, GRAPPA acceleration factor = 2). T2-weighted T2-SPACE images were obtained (TR = 3200 ms TE = 563 ms, FOV = 256 × 240, 0.8 mm isotropic voxel size, 208 slices). A standard fieldmap (TR = 731 ms, TE = 4.92/7.38, FOV = 208 × 180,

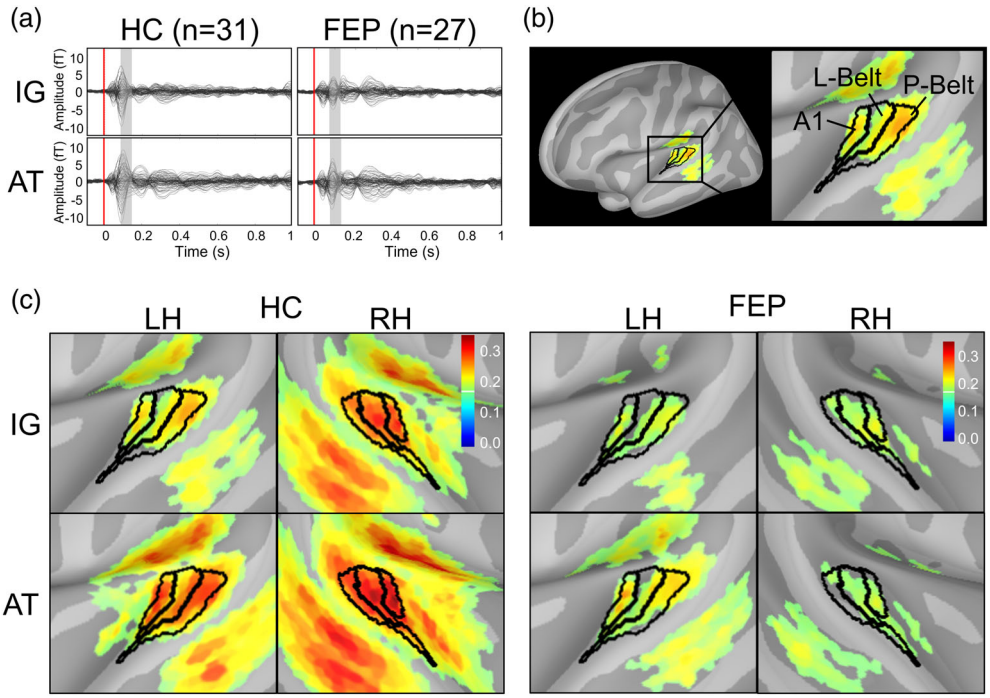

FIGURE 2 Impaired auditory cortex attention modulation in first-episode psychosis (FEP). (a) The M100 modulation time window (80–140 ms) is highlighted in the butterfly plot of magnetometer sensors. (b) The M100 response to tones in healthy controls during the ignore condition. The auditory cortex regions of interest defined by the Human Connectome Project multimodal parcellation (HCP-MMP) include bilateral primary auditory cortex (A1), lateral belt (LBelt), and parabelt (PBelt) (only left hemisphere shown for reference). (c) Cortical source activity (dynamic statistical parametric maps [dSPM]) averaged over 80–140 ms. Within A1, LBelt, and PBelt, FEP have overall less activity and are impaired in the ability to enhance activity with attention.

2.0 mm voxel size, 72 slices) was collected for correcting readout distortion in the T1w and T2w images. Ten minutes of eyes-open (passive crosshair viewing) resting state BOLD fMRI data were acquired using a multiband pulse sequence (TR = 800 ms, TE = 37 ms, multiband factor = 8, flip angle = 52°, FOV = 208 × 208 mm, voxel size = 2.0 mm^3, 72 slices). A single-band reference image with no slice acceleration was acquired at the beginning of each run to improve registrations. Finally, two spin echo EPI images (TR = 8000 ms, TE = 66 ms, flip angle = 90, FOV = 208 × 208 mm, 2.0 mm voxel size, 72 slices) with reversed phase encoding directions were acquired. MRI data were collected as a separate session from the MEG data, which was typically on a separate day (between session mean = 9.9 ± 10.2 days, median = 7 days, range = 0–48 days).

The publicly available HCP-pipelines (https://github.com/Washington-University/HCPpipelines) were used for MRI processing (detailed in Glasser et al., 2013). Briefly, the structural images were corrected for gradient nonlinearity, readout, and bias field, followed by AC–PC alignment. Myelin maps were created by dividing the T1w image by the T2w image. Native space images were used to generate white and pial surfaces with FreeSurfer and were refined using T2w data. Then, the individual's native-mesh surfaces were registered with a MSM algorithm with MSMsulc to the Conte69 folding-based template (Robinson et al., 2014; Van Essen et al., 2012).

The functional resting-state data were collected with the structural MRI and processed with the HCP pipelines, which utilize the fMRI data with MSMall algorithm to improve registration and alignment between participants. fMRI data were first corrected for gradient-nonlinearity. A six DOF FLIRT registration of each frame to the single-band reference image was used to correct for motion. The reverse phase spin-echo images were used to correct functional distortion. The single band reference image was registered to the T1w image with FreeSurfer's BBRegister (Greve & Fischl, 2009). All the transforms and distortion correction were applied in a single resampling step. The data were brain masked and intensity normalized to a 4D whole brain mean of 10,000. Then, a voxel to surface mapping was performed to sample the volumetric fMRI data to the individual's native surfaces, which were subsequently resampled to a standard 32k fs_LR surface. The ICA + FIX pipeline was used to generate resting-state ICA component spatial maps and timeseries and to remove artifactual noise (Griffanti et al., 2014; Salimi-Khorshidi et al., 2014).

Resting-state network component maps were calculated with a weighted spatial multiple regression implemented in the HCP pipelines. Briefly, this method is an adaptation from dual regression which utilizes spatial and temporal regression to find individual component maps from group maps. In Step 1, a spatial group map of a network, provided in the HCP pipelines, was used as a spatial regressor to identify the individual-specific timeseries associated with the group map vertices. A spatial weighting map was included that compensates for distortion between the individual's native space and standard space

and includes upweighting for regions likely to be well aligned. In Step 2, these timeseries were regressed (as temporal regressors) in the same individual's dataset to identify all vertices in the individual associated with that timeseries. Finally, to refine the individual's spatial maps, the two steps were repeated. In the second round of Step 1, the individual participant component spatial maps were used to regress the individual timeseries associated with those vertices. Then, this timeseries was used as a temporal regressor to identify all vertices in the individual associated with the timeseries. The HCP pipelines also utilized fMRI connectivity maps from primary visual cortex (V1). A similar regression method was used to calculate the visuotopic resting fMRI functional connectivity maps. The V1 spatial regressors, based on published maps of eccentricity and polar angle in V1, were spatially regressed into the individual's timeseries to identify the timeseries associated the regressors. Then, these time courses were temporally regressed in the individual's timeseries to generate whole brain spatial maps in each of the individuals. Finally, the HCP MSMAll pipeline was utilized to register individuals to a group average atlas surface using a two-stage process based on the MSM algorithm (Robinson et al., 2014). The first stage was driven by cortical folding patterns (FreeSurfer's "sulc" measure), and the second stage utilized cortical areal features (myelin, resting-state network maps, and visuospatial topographic maps) (for details, see Glasser et al., 2016).

The group average HCP-MMP was applied to individuals' MRI data and mapped to individuals' cortical surface in native space in FreeSurfer (https://wiki.humanconnectome.org/display/PublicData/HCP+Users+FAQ#HCPUsersFAQ-9.HowdoImapdatabetweenFreeSurferandHCP?). In the connectome workbench, a dense-label file was created for each individual from the group average HCP-MMP and converted to GIFTI format, which was resampled to fsaverage space. In FreeSurfer, this file was converted to an annotation file and resampled to the individual participant's surface. These individual cortical surfaces, along with the corresponding HCP-MMP, were imported to Brainstorm to be registered with the MEG activity for the ROI source analysis (see MEG methods and supplementary materials).

2.5 | Analysis

Group demographics were compared using independent samples *t* test and chi-square tests where appropriate. MEG sensor data were used to visualize the event-related fields and were not compared with statistical analysis. Source activity was compared using repeated measures ANOVA with one between-subjects factor (group: FEP or control) and three within-subject factors (attention: attend or ignore, hemisphere: left or right, and region: A1, LBelt, PBelt). Simple effects were examined using follow-up one-way between-subjects ANOVA or repeated-measures ANOVA, as appropriate. An exploratory analysis was performed to investigate potential M100 modulation differences between FEP who later received a diagnosis on the schizophrenia spectrum and FEP who later received a diagnosis of an affective disorder (bipolar and major depression).

Exploratory correlations of attention modulated source activity (attend-ignore) with symptom scores (PANSS total, PANSS positive, and PANSS negative), cognitive measures (MCCB composite *t* score, WASI Vocab), and social functioning (global functioning: role, global functioning: social) were assessed with Spearman's correlations. Results were considered significant at $p < .05$.

With the large number of individual items and need for multiple comparisons correction, associations were first examined at broader symptom groupings, then if the factors were significant, individual items within that factor was assessed.

3 | RESULTS

3.1 | Sensor level data

MEG sensor level data were segmented and averaged to produce the event-related field. Average magnetometer sensor waveforms for HC and FEP are shown in Figure 2a, with M100 time-window (80–140 ms) indicated by the shaded bar. The sensor level data were not analyzed, but it is presented to demonstrate validity of the morphology of the event-related field and indicate the time-window of interest from which cortical source activity, the central measure of interest, is derived.

3.2 | Cortical source data

Submillimeter resolution structural MRI scans were obtained from all participants and processed with the HCP processing protocols. This allows for the most accurate registration of the HCP cortical parcellation, with heretofore unavailable identification of functional cortical areas. Figure 2b shows the left hemisphere source map of M100 response in HC, demonstrating the strongest M100 source activity is primarily found in auditory cortex. Delineation of A1, lateral belt (LBelt), and parabelt (PBelt) are shown in Figure 2b.

MEG sensor data were registered to individual MRIs, and cortical activity was calculated using minimum norm estimation and normalized to the noise covariance with dSPM. The source activity averaged across the ROIs are shown in Figure 2c and means and SD are reported in Table 2. Overall, FEP exhibited significantly reduced activity compared with HC over the 80- to 140-ms time window ($F(1,56) = -7.41$, $p = .009$, $\eta_p^2 = .117$), indicating a broad sensory deficit. Of primary importance, there was a significant interaction between group and attention ($F(1,56) = 4.10$, $p = .048$, $\eta_p^2 = .068$), where HC enhanced source activity with attention ($F(1,30) = 11.64$, $p = .002$, $\eta_p^2 = .280$), but FEP did not ($F(1,26) = 0.80$, $p = .379$, $\eta_p^2 = .030$). Attention modulation differed between hemispheres ($F(1,56) = 4.41$, $p = .040$, $\eta_p^2 = .073$), as the left hemisphere showed significant M100 attention modulation ($F(1,56) = 11.45$, $p = .001$, $\eta_p^2 = .170$), while the right hemisphere did not ($F(1,56) = 1.86$, $p = .178$, $\eta_p^2 = .032$). This interaction did not differ between FEP and HC ($F(1,56) = 0.04$, $p = .947$, $\eta_p^2 < .001$). There were no significant

TABLE 2 *Cortical source activity*. Averaged dSPM source values (Mean ± SD) across the 80–140 ms time window within each auditory cortex ROI

	FEP		HC	
	Attend	Ignore	Attend	Ignore
Left A1	0.20 ± 0.11	0.19 ± 0.08	0.27 ± 0.17	0.21 ± 0.13
Left LBelt	0.19 ± 0.10	0.17 ± 0.08	0.24 ± 0.16	0.20 ± 0.13
Left PBelt	0.21 ± 0.11	0.19 ± 0.09	0.25 ± 0.15	0.21 ± 0.13
Right A1	0.18 ± 0.11	0.19 ± 0.08	0.30 ± 0.17	0.28 ± 0.14
Right LBelt	0.18 ± 0.09	0.19 ± 0.08	0.30 ± 0.15	0.27 ± 0.14
Right PBelt	0.16 ± 0.08	0.16 ± 0.07	0.27 ± 0.15	0.24 ± 0.12

Abbreviations: dSPM, dynamic statistical parametric maps; FEP, first-episode psychosis; HC, healthy control.

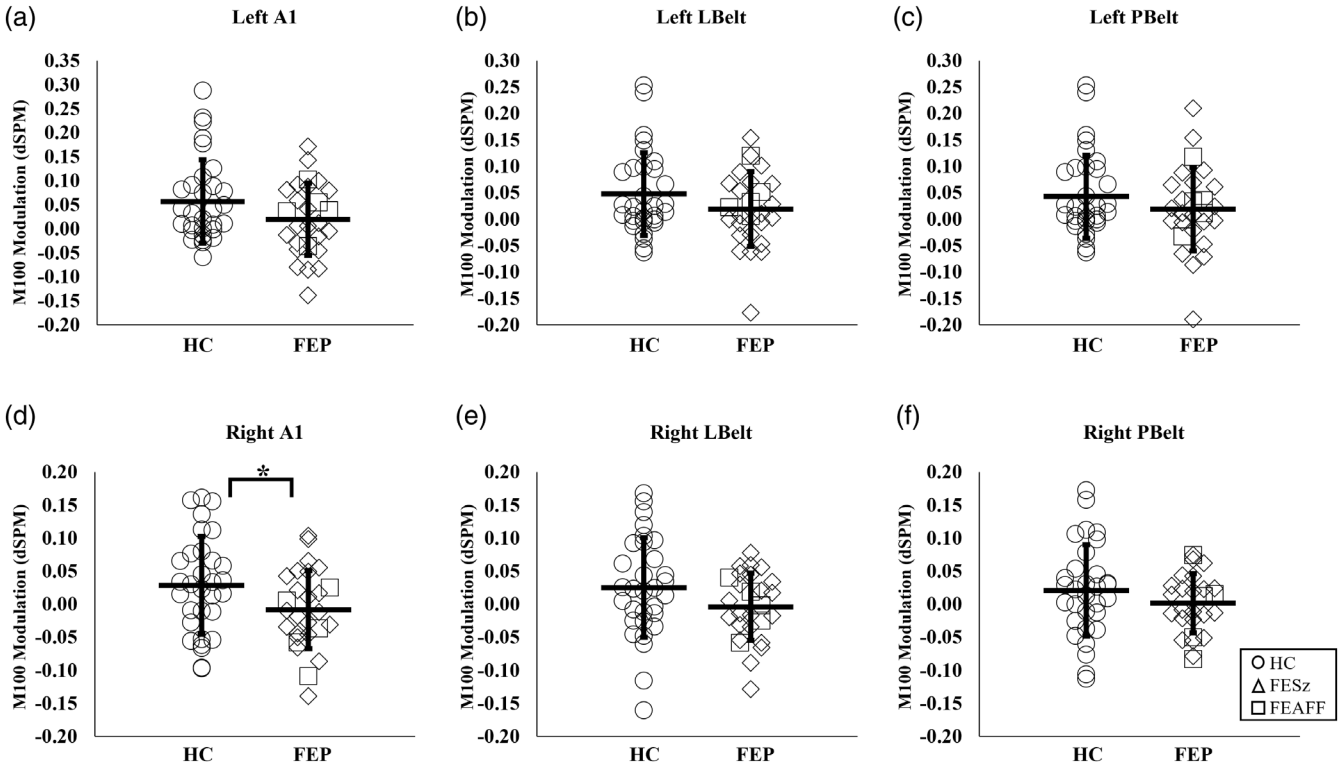

FIGURE 3 Scatterplots of the M100 modulation group differences in auditory cortex regions. Compared to healthy individuals, first-episode psychosis (FEP) experienced general deficits in the ability to modulate the M100 with attention across all regions of interest (a–f). There was a significant group difference between HC and FEP in the right A1 (* denotes $p < .05$). FEP with a schizophrenia spectrum diagnosis (FESz) are identified separately from those with an affective disorder diagnosis (FEAFF). There were no significant differences between FESz and FEAFF

interaction with region ($F(2,112) = 0.11$, $p = .898$, $\eta_p^2 = .004$), suggesting relatively widespread deficits across several early auditory cortex regions. Attention modulation values and individual *t*-test statistics with effect sizes (Hedges' g) and confidence intervals for each individual region of interest are reported in Supplemental Table S2.

The exploratory analysis of differences between individuals with a diagnosis of schizophrenia spectrum and those with a diagnosis of an affective disorder (bipolar and major depression), revealed no significant interaction with diagnostic group ($F(1,25) = 0.06$, $p = .805$, $\eta_p^2 = .002$) (Figure 3).

3.3 | Exploratory correlations with clinical and cognitive measures

There were no significant correlations with differential source activity in FEP (*p*'s > .05). In HC, only left A1 modulation was negatively associated with WASI Vocab scores ($\rho = -0.36$, $p = .045$). With no significant correlation with symptom factor scores, the analysis was precluded from investigating relationships with individual items. Nonetheless, to capitalize on the wealth of clinical symptom data acquired, relationships with each individual PANSS item are reported in Supplemental Tables S3 and S4 for the interested reader.

4 | DISCUSSION

This is the first demonstration that increases in sensory M100 gain localize to A1 and auditory belt parcels, and FEP experience both sensory and attentional gain modulation deficits in these specific auditory cortex parcels. This aligns with and improves the previous understanding of specific sources, as previous reports suggested M100 enhancement with attention generally localized to auditory cortex (Ahveninen et al., 2006; Petkov et al., 2004). Previous MEG studies source localizing the M100 have localized activity to Heschl's gyrus, planum temporale, and superior temporal gyrus (Ahveninen et al., 2006; Woldorff et al., 1993). This aligns with attention modulation evidence from other imaging modalities. Functional MRI activation increases in both primary and nonprimary auditory cortex during auditory attention tasks (Grady et al., 1997; Jancke et al., 1999; Rinne et al., 2007). Similarly, PET studies have demonstrated regional cerebral blood flow increases in auditory cortex with attention (Alho et al., 2003; Zatorre et al., 1999). However, here we improved the specificity of defining this auditory attention enhancement by localizing it to more specific subregions of the auditory cortex, A1, and auditory belt parcels. Primary auditory cortex, lateral belt, and parabelt, reside in Heschl's gyrus and planum temporale, both in turn are part of superior temporal gyrus. These parcels have clear correspondence between the human A1 (and belt) and animal A1 (and belt) regions (Sweet et al., 2005). Thus, this knowledge can be more readily moved into model systems, such as the monkey or ferret to further elucidate underlying auditory attention mechanisms within these regions. The ferret has become a valuable animal model to understanding the neurobiology of auditory system, particularly understanding the neural basis for selective attention at multiple hierarchical levels in auditory cortex (Elgueda et al., 2019). This study provides an important translational step between human and animal models.

Individuals at their FEP experienced sensory and attention impairments in these auditory regions. It was previously found that FEP has an impaired sensory EEG-recorded N100 in addition to an impaired ability to modulate the N100 amplitude with attention (Ren et al., 2021). However, the cortical regions underlying this deficit remained unknown. Here, we showed that FEP had reduced sensory activity in both primary and nonprimary auditory cortex bilaterally. Further, FEP were deficient in enhancing cortical activity with attention across these regions as well, suggesting that they have relatively widespread sensory and attention modulation deficits in auditory cortex, encompassing primary and nonprimary auditory cortex. The specificity of localizing this functional deficit in primary and auditory belt regions may provide insight to the emergence of psychosis, as specific temporal lobe abnormalities (e.g., Heschl's gyrus gray matter reduction) are present very early in the disorder (Curtis et al., 2021; Kasai et al., 2003) and show progressive pathology with disease duration (Salisbury et al., 2007). Understanding how the underlying progressive pathology relates to decline in functional abilities such as auditory attention modulation can provide a better understanding of this interplay at the emergence of psychosis. Future longitudinal analyses in combination with structural gray matter/white matter information can address this directly. Further, this study provides specific target areas for therapies to modulate activity using NIBS, such as transcranial direct stimulation or repetitive transcranial magnetic stimulation. Interventions initiated early in the disease improve functional outcome and reduce long-term treatment costs (Eack et al., 2010; Kane et al., 2016; Srihari et al., 2012). These early interventions would improve from a more precise understanding of the specific cortical regions to engage during treatment.

As a follow-up to previous work on the N100 attention modulation in FEP and informed from previous source localization of the M100, this work was limited to a specific hypothesis-driven analysis of auditory cortex activity within the time window the M100 attention modulation. While there is a distinct deficit within these auditory regions, it is unclear if this impairment is restricted to auditory cortex or is due to an inability of long-range cortical communication from frontal cortex to modulate activity within auditory cortex. Previously, the N100 enhancement was related to functions that involve the frontal executive network (e.g., cognition, negative symptoms, and social functioning) (Ren et al., 2021). The general executive attention network includes the prefrontal cortex, posterior parietal cortex, and sensory areas (Hopfinger et al., 2000; Petersen & Posner, 2012; Tobyne et al., 2017). While fMRI provides ample evidence for general auditory attention network, the dynamics underlying modulation of the N100/M100 with attention are unknown. Attention is related to increased gamma band synchrony in sensory areas, and this appears to be coordinated from PFC (Gregoriou et al., 2009; Gregoriou et al., 2012). The long-range synchrony is likely mediated by a low carrier frequency (theta/alpha), as sensory gamma oscillations become organized by alpha modulations in the PFC (Spaak et al., 2012). In the auditory cortex, it may likely be mediated by theta band oscillations, as phase amplitude coupling in the auditory cortex is primarily observed between the theta and gamma amplitude (Doesburg et al., 2012; Lizarazu et al., 2019; Murphy et al., 2020). There has been little study of oscillatory mechanisms associated with attentional impairments in psychosis, with one MEG study showing decreased alpha desynchrony in schizophrenia in the context of an oddball task (Koh et al., 2011) and others showing intact phase-amplitude coupling in schizophrenia during auditory steady state stimulation (Kirihara et al., 2012; Murphy et al., 2020). Future work will extend this investigation to understand functional connectivity with auditory-executive frontal cortex that may mediate this attentional modulation deficit.

The current study is the first to provide crucial insight into the specific cortical areas involved in auditory attentional gain modulation in HC and into the sensory and early attention deficits in FEP. The novel use of the HCP-MMP revealed the precise cortical areas underlying attention modulation and impairments in FEP, providing an understanding critical for translational study and for potential early interventions. The M100 sensory reduction and failure to modulate with selective attention may indicate local and systems-level pathophysiology proximal to disease onset that may be critical for etiology.

AUTHOR CONTRIBUTIONS

Dean F. Salisbury designed the study, interpreted findings, and contributed to the critical revision of the manuscript. Mark T. Curtis, Brian A. Coffman, and Xi Ren helped collect data. Mark T. Curtis performed

literature searches and wrote the first draft of the manuscript. Mark T. Curtis performed analyses with the aid and instruction of Brian A. Coffman and Xi Ren. All authors have approved the final manuscript.

ACKNOWLEDGMENTS

This work was supported by National Institute of Mental Health R01 MH108568 (DFS), RO1 MH113533 (DFS), and F31 MH119718 (MTC). The authors thank the faculty and staff of the WPH Psychosis Recruitment and Assessment Core, the Conte Center for Translational Mental Health Research (P50 MH103204, David Lewis, MD, Director), and the University of Pittsburgh Clinical Translational Science Institute (UL1 RR024153, Steven E. Reis, MD) for their assistance in recruitment, diagnostic and psychopathological assessments, and neuropsychological evaluations. The authors would also like to thank Vanessa Fishel, Natasha Torrence, Yiming Wang, Dylan Seebold, Rebekah Farris, Timothy Murphy, Justin Leiter, and Maria Jalbrzikowski, PhD, for their assistance in collecting the MEG and MRI data.

CONFLICT OF INTEREST

The authors declare no conflicts of interest.

DATA AVAILABILITY STATEMENT

The data that support the findings of this study are available upon request from the corresponding author and in the NIH RDoC database.

CONSENT STATEMENT

All participants provided informed consent and were paid for participation.

ORCID

Mark T. Curtis https://orcid.org/0000-0002-0467-7321
Brian A. Coffman https://orcid.org/0000-0001-9374-5105
Dean F. Salisbury https://orcid.org/0000-0002-8533-0599

REFERENCES

Ahveninen, J., Jaaskelainen, I. P., Raij, T., Bonmassar, G., Devore, S., Hamalainen, M., Levanen, S., Lin, F.H., Sams, M., & Belliveau, J. W. (2006). Task-modulated "what" and "where" pathways in human auditory cortex. *Proceedings of the National Academy of Sciences of the United States of America*, *103*(39), 14608–14613. https://doi.org/10.1073/pnas.0510480103

Alho, K., Vorobyev, V. A., Medvedev, S. V., Pakhomov, S. V., Roudas, M. S., Tervaniemi, M., van Zuijen, T., & Naatanen, R. (2003). Hemispheric lateralization of cerebral blood-flow changes during selective listening to dichotically presented continuous speech. *Brain Research. Cognitive Brain Research*, *17*(2), 201–211. https://doi.org/10.1016/s0926-6410(03)00091-0

Bilder, R. M., Degreef, G., Pandurangi, A. K., Rieder, R. O., Sackeim, H. A., & Mukherjee, S. (1988). Neuropsychological deterioration and CT scan findings in chronic schizophrenia. *Schizophrenia Research*, *1*(1), 37–45. https://doi.org/10.1016/0920-9964(88)90038-2

Caspi, A., Reichenberg, A., Weiser, M., Rabinowitz, J., Kaplan, Z., Knobler, H., Davidson-Sagi, N., & Davidson, M. (2003). Cognitive performance in schizophrenia patients assessed before and following the first psychotic episode. *Schizophrenia Research*, *65*(2–3), 87–94.

Coalson, T. S., Van Essen, D. C., & Glasser, M. F. (2018). The impact of traditional neuroimaging methods on the spatial localization of cortical areas. *Proceedings of the National Academy of Sciences of the United States of America*, *115*(27), E6356–E6365. https://doi.org/10.1073/pnas.1801582115

Cornblatt, B. A., Lencz, T., Smith, C. W., Correll, C. U., Auther, A. M., & Nakayama, E. (2003). The schizophrenia prodrome revisited: A neurodevelopmental perspective. *Schizophrenia Bulletin*, *29*(4), 633–651.

Curtis, M. T., Coffman, B. A., & Salisbury, D. F. (2021). Pitch and duration mismatch negativity are associated with distinct auditory cortex and inferior frontal cortex volumes in the First-episode schizophrenia Spectrum. *Schizophrenia Bulletin Open*, *2*(1), sgab005. https://doi.org/10.1093/schizbullopen/sgab005

de Oliveira, M. O., Nitrini, R., Yassuda, M. S., & Brucki, S. M. (2014). Vocabulary is an appropriate measure of premorbid intelligence in a sample with heterogeneous educational level in Brazil. *Behavioural Neurology*, *2014*, 875960. https://doi.org/10.1155/2014/875960

Delorme, A., & Makeig, S. (2004). EEGLAB: An open source toolbox for analysis of single-trial EEG dynamics including independent component analysis. *Journal of Neuroscience Methods*, *134*(1), 9–21. https://doi.org/10.1016/j.jneumeth.2003.10.009

Doesburg, S. M., Green, J. J., McDonald, J. J., & Ward, L. M. (2012). Theta modulation of inter-regional gamma synchronization during auditory attention control. *Brain Research*, *1431*, 77–85. https://doi.org/10.1016/j.brainres.2011.11.005

Eack, S. M., Hogarty, G. E., Cho, R. Y., Prasad, K. M., Greenwald, D. P., Hogarty, S. S., & Keshavan, M. S. (2010). Neuroprotective effects of cognitive enhancement therapy against gray matter loss in early schizophrenia: Results from a 2-year randomized controlled trial. *Archives of General Psychiatry*, *67*(7), 674–682. https://doi.org/10.1001/archgenpsychiatry.2010.63

Eberhard, J., Riley, F., & Levander, S. (2003). Premorbid IQ and schizophrenia. Increasing cognitive reduction by episodes. *European Archives of Psychiatry and Clinical Neuroscience*, *253*(2), 84–88. https://doi.org/10.1007/s00406-003-0412-y

Elgueda, D., Duque, D., Radtke-Schuller, S., Yin, P., David, S. V., Shamma, S. A., & Fritz, J. B. (2019). State-dependent encoding of sound and behavioral meaning in a tertiary region of the ferret auditory cortex. *Nature Neuroscience*, *22*(3), 447–459. https://doi.org/10.1038/s41593-018-0317-8

Fett, A. K., Viechtbauer, W., Dominguez, M. D., Penn, D. L., van Os, J., & Krabbendam, L. (2011). The relationship between neurocognition and social cognition with functional outcomes in schizophrenia: A meta-analysis. *Neuroscience and Biobehavioral Reviews*, *35*(3), 573–588. https://doi.org/10.1016/j.neubiorev.2010.07.001

First, M. B., Spitzer, R. L., Gibbon, M., & Williams, J. (1997). *Structured clinical interview for DSM-IV axis I disorders*. Biometrics Research Department.

Foxe, J. J., Yeap, S., Snyder, A. C., Kelly, S. P., Thakore, J. H., & Molholm, S. (2011). The N1 auditory evoked potential component as an endophenotype for schizophrenia: High-density electrical mapping in clinically unaffected first-degree relatives, first-episode, and chronic schizophrenia patients. *European Archives of Psychiatry and Clinical Neuroscience*, *261*(5), 331–339. https://doi.org/10.1007/s00406-010-0176-0

Fritz, J., Shamma, S., Elhilali, M., & Klein, D. (2003). Rapid task-related plasticity of spectrotemporal receptive fields in primary auditory cortex. *Nature Neuroscience*, *6*(11), 1216–1223. https://doi.org/10.1038/nn1141

Glasser, M. F., Coalson, T. S., Robinson, E. C., Hacker, C. D., Harwell, J., Yacoub, E., Ugurbil, K., Andersson, J., Beckmann, C. F., Jenkinson, M., Smith, S. M., & Van Essen, D. C. (2016). A multi-modal parcellation of human cerebral cortex. *Nature*, *536*(7615), 171–178. https://doi.org/10.1038/nature18933

Glasser, M. F., Sotiropoulos, S. N., Wilson, J. A., Coalson, T. S., Fischl, B., Andersson, J. L., Xu, J., Jbabdi, S., Webster, M., Polimeni, J. R., Van Essen, D. C., & Jenkinson, M. (2013). The minimal preprocessing pipelines for the Human Connectome Project. *NeuroImage*, *80*, 105–124. https://doi.org/10.1016/j.neuroimage.2013.04.127

Grady, C. L., Van Meter, J. W., Maisog, J. M., Pietrini, P., Krasuski, J., & Rauschecker, J. P. (1997). Attention-related modulation of activity in primary and secondary auditory cortex. *Neuroreport*, *8*(11), 2511–2516. https://doi.org/10.1097/00001756-199707280-00019

Gregoriou, G. G., Gotts, S. J., & Desimone, R. (2012). Cell-type-specific synchronization of neural activity in FEF with V4 during attention. *Neuron*, *73*(3), 581–594. https://doi.org/10.1016/j.neuron.2011.12.019

Gregoriou, G. G., Gotts, S. J., Zhou, H., & Desimone, R. (2009). High-frequency, long-range coupling between prefrontal and visual cortex during attention. *Science*, *324*(5931), 1207–1210. https://doi.org/10.1126/science.1171402

Greve, D. N., & Fischl, B. (2009). Accurate and robust brain image alignment using boundary-based registration. *NeuroImage*, *48*(1), 63–72. https://doi.org/10.1016/j.neuroimage.2009.06.060

Griffanti, L., Salimi-Khorshidi, G., Beckmann, C. F., Auerbach, E. J., Douaud, G., Sexton, C. E., Zsoldos, E., Ebmeier, K. P., Filippini, N., Mackay, C. E., Moeller, S., Xu, J., Yacoub, E., Baselli, G., Ugurbil, K., Miller, K. L., & Smith, S. M. (2014). ICA-based artefact removal and accelerated fMRI acquisition for improved resting state network imaging. *NeuroImage*, *95*, 232–247. https://doi.org/10.1016/j.neuroimage.2014.03.034

Heaton, R. K., Gladsjo, J. A., Palmer, B. W., Kuck, J., Marcotte, T. D., & Jeste, D. V. (2001). Stability and course of neuropsychological deficits in schizophrenia. *Archives of General Psychiatry*, *58*(1), 24–32. https://doi.org/10.1001/archpsyc.58.1.24

Hillyard, S. A., Hink, R. F., Schwent, V. L., & Picton, T. W. (1973). Electrical signs of selective attention in the human brain. *Science*, *182*(4108), 177–180.

Hoff, A. L., Sakuma, M., Wieneke, M., Horon, R., Kushner, M., & DeLisi, L. E. (1999). Longitudinal neuropsychological follow-up study of patients with first-episode schizophrenia. *The American Journal of Psychiatry*, *156*(9), 1336–1341. https://doi.org/10.1176/ajp.156.9.1336

Hopfinger, J. B., Buonocore, M. H., & Mangun, G. R. (2000). The neural mechanisms of top-down attentional control. *Nature Neuroscience*, *3*(3), 284–291. https://doi.org/10.1038/72999

Jancke, L., Mirzazade, S., & Shah, N. J. (1999). Attention modulates activity in the primary and the secondary auditory cortex: A functional magnetic resonance imaging study in human subjects. *Neuroscience Letters*, *266*(2), 125–128. https://doi.org/10.1016/s0304-3940(99)00288-8

Kane, J. M., Robinson, D. G., Schooler, N. R., Mueser, K. T., Penn, D. L., Rosenheck, R. A., Addington, J., Brunette, M. F., Correll, C. U., Estroff, S. E., Marcy, P., Robinson, J., Meyer-Kalos, P. S., Gottlieb, J. D., Glynn, S. M., Lynde, D. W., Pipes, R., Kurian, B. T., Miller, A. L., … Heinssen, R. K. (2016). Comprehensive versus usual community care for first-episode psychosis: 2-year outcomes from the NIMH RAISE Early Treatment Program. *The American Journal of Psychiatry*, *173*(4), 362–372. https://doi.org/10.1176/appi.ajp.2015.15050632

Kasai, K., Shenton, M. E., Salisbury, D. F., Hirayasu, Y., Onitsuka, T., Spencer, M. H., Yurgelun-Todd, D. A., Kikinis, R., Jolesz, F. A., & McCarley, R. W. (2003). Progressive decrease of left Heschl gyrus and planum temporale gray matter volume in first-episode schizophrenia: A longitudinal magnetic resonance imaging study. *Archives of General Psychiatry*, *60*(8), 766–775. https://doi.org/10.1001/archpsyc.60.8.766

Kay, S. R., Fiszbein, A., & Opler, L. A. (1987). The Positive and Negative Syndrome Scale (PANSS) for schizophrenia. *Schizophrenia Bulletin*, *13*(2), 261–276. https://doi.org/10.1093/schbul/13.2.261

Kern, R. S., Gold, J. M., Dickinson, D., Green, M. F., Nuechterlein, K. H., Baade, L. E., Keefe, R. S. E., Mesholam-Gately, R. I., Seidman, L. J., Lee, C., Sugar, C. A., & Marder, S. R. (2011). The MCCB impairment profile for schizophrenia outpatients: Results from the MATRICS psychometric and standardization study. *Schizophrenia Research*, *126*(1–3), 124–131. https://doi.org/10.1016/j.schres.2010.11.008

Kirihara, K., Rissling, A. J., Swerdlow, N. R., Braff, D. L., & Light, G. A. (2012). Hierarchical organization of gamma and theta oscillatory dynamics in schizophrenia. *Biological Psychiatry*, *71*(10), 873–880. https://doi.org/10.1016/j.biopsych.2012.01.016

Koh, Y., Shin, K. S., Kim, J. S., Choi, J. S., Kang, D. H., Jang, J. H., Cho, K. H., O'Donnell, B. F., Chung, C. K., & Kwon, J. S. (2011). An MEG study of alpha modulation in patients with schizophrenia and in subjects at high risk of developing psychosis. *Schizophrenia Research*, *126*(1–3), 36–42. https://doi.org/10.1016/j.schres.2010.10.001

Kraepelin, E. (1889). *Psychiatrie: Ein lehrbuch für studirende und aerzte* (3rd ed.). Abel.

Kremen, W. S., Seidman, L. J., Faraone, S. V., Pepple, J. R., Lyons, M. J., & Tsuang, M. T. (1995). The '3 Rs' and neuropsychological function in schizophrenia: A test of the matching fallacy in biological relatives. *Psychiatry Research*, *56*(2), 135–143. https://doi.org/10.1016/0165-1781(94)02652-1

Lizarazu, M., Lallier, M., & Molinaro, N. (2019). Phase-amplitude coupling between theta and gamma oscillations adapts to speech rate. *Annals of the New York Academy of Sciences*, *1453*(1), 140–152. https://doi.org/10.1111/nyas.14099

Luck, S. J., Chelazzi, L., Hillyard, S. A., & Desimone, R. (1997). Neural mechanisms of spatial selective attention in areas V1, V2, and V4 of macaque visual cortex. *Journal of Neurophysiology*, *77*(1), 24–42. https://doi.org/10.1152/jn.1997.77.1.24

McAdams, C. J., & Reid, R. C. (2005). Attention modulates the responses of simple cells in monkey primary visual cortex. *The Journal of Neuroscience*, *25*(47), 11023–11033. https://doi.org/10.1523/JNEUROSCI.2904-05.2005

Mohn-Haugen, C. R., Mohn, C., Laroi, F., Teigset, C. M., Oie, M. G., & Rund, B. R. (2022). A systematic review of premorbid cognitive functioning and its timing of onset in schizophrenia spectrum disorders. *Schizophrenia Research: Cognition*, *28*, 100246. https://doi.org/10.1016/j.scog.2022.100246

Murphy, N., Ramakrishnan, N., Walker, C. P., Polizzotto, N. R., & Cho, R. Y. (2020). Intact auditory cortical cross-frequency coupling in early and chronic schizophrenia. *Frontiers in Psychiatry*, *11*, 507. https://doi.org/10.3389/fpsyt.2020.00507

Neelon, M. F., Williams, J., & Garell, P. C. (2006). The effects of auditory attention measured from human electrocorticograms. *Clinical Neurophysiology*, *117*(3), 504–521. https://doi.org/10.1016/j.clinph.2005.11.009

Nuechterlein, K. H., Green, M. F., Kern, R. S., Baade, L. E., Barch, D. M., Cohen, J. D., Essock, S., Fenton, W. S., Frese, F. J., 3rd, Gold, J. M., Goldberg, T., Heaton, R. K., Keef, R. S., Kraemer, H., Mesholam-Gately, R., Seidman, L. J., Stover, E., Weinberger, D. R., Young, A. S., … Marder, S. R. (2008). The MATRICS consensus cognitive battery, part 1: Test selection, reliability, and validity. *The American Journal of Psychiatry*, *165*(2), 203–213. https://doi.org/10.1176/appi.ajp.2007.07010042

O'Donnell, B. F., Hokama, H., McCarley, R. W., Smith, R. S., Salisbury, D. F., Mondrow, E., Nestor, P. G., & Shenton, M. E. (1994). Auditory ERPs to non-target stimuli in schizophrenia: Relationship to probability, task-demands, and target ERPs. *International Journal of Psychophysiology*, *17*(3), 219–231.

Parasuraman, R. (1985). Event-related brain potentials and intermodal divided attention. *Proceedings of the Human Factors and Ergonomics Society Annual Meeting*, *29*, 971–975.

Petersen, S. E., & Posner, M. I. (2012). The attention system of the human brain: 20 years after. *Annual Review of Neuroscience*, *35*, 73–89. https://doi.org/10.1146/annurev-neuro-062111-150525

Petkov, C. I., Kang, X., Alho, K., Bertrand, O., Yund, E. W., & Woods, D. L. (2004). Attentional modulation of human auditory cortex. *Nature Neuroscience*, *7*(6), 658–663. https://doi.org/10.1038/nn1256

Ren, X., Fribance, S. N., Coffman, B. A., & Salisbury, D. F. (2021). Deficits in attentional modulation of auditory N100 in first-episode schizophrenia. *The European Journal of Neuroscience*, *53*, 2629–2638. https://doi.org/10.1111/ejn.15128

Rinne, T., Stecker, G. C., Kang, X., Yund, E. W., Herron, T. J., & Woods, D. L. (2007). Attention modulates sound processing in human auditory cortex but not the inferior colliculus. *Neuroreport*, *18*(13), 1311–1314. https://doi.org/10.1097/WNR.0b013e32826fb3bb

Robinson, E. C., Jbabdi, S., Glasser, M. F., Andersson, J., Burgess, G. C., Harms, M. P., Smith, S. M., Van Essen, D. C., & Jenkinson, M. (2014). MSM: A new flexible framework for multimodal surface matching. *NeuroImage*, *100*, 414–426. https://doi.org/10.1016/j.neuroimage.2014.05.069

Rosburg, T., Boutros, N. N., & Ford, J. M. (2008). Reduced auditory evoked potential component N100 in schizophrenia—A critical review. *Psychiatry Research*, *161*(3), 259–274. https://doi.org/10.1016/j.psychres.2008.03.017

Salimi-Khorshidi, G., Douaud, G., Beckmann, C. F., Glasser, M. F., Griffanti, L., & Smith, S. M. (2014). Automatic denoising of functional MRI data: Combining independent component analysis and hierarchical fusion of classifiers. *NeuroImage*, *90*, 449–468. https://doi.org/10.1016/j.neuroimage.2013.11.046

Salisbury, D. F., Collins, K. C., & McCarley, R. W. (2010). Reductions in the N1 and P2 auditory event-related potentials in first-hospitalized and chronic schizophrenia. *Schizophrenia Bulletin*, *36*(5), 991–1000. https://doi.org/10.1093/schbul/sbp003

Salisbury, D. F., Kuroki, N., Kasai, K., Shenton, M. E., & McCarley, R. W. (2007). Progressive and interrelated functional and structural evidence of post-onset brain reduction in schizophrenia. *Archives of General Psychiatry*, *64*(5), 521–529. https://doi.org/10.1001/archpsyc.64.5.521

Spaak, E., Bonnefond, M., Maier, A., Leopold, D. A., & Jensen, O. (2012). Layer-specific entrainment of γ-band neural activity by the α rhythm in monkey visual cortex. *Current Biology*, *22*(24), 2313–2318. https://doi.org/10.1016/j.cub.2012.10.020

Spitzer, H., Desimone, R., & Moran, J. (1988). Increased attention enhances both behavioral and neuronal performance. *Science*, *240*(4850), 338–340.

Srihari, V. H., Shah, J., & Keshavan, M. S. (2012). Is early intervention for psychosis feasible and effective? *The Psychiatric Clinics of North America*, *35*(3), 613–631. https://doi.org/10.1016/j.psc.2012.06.004

Sweet, R. A., Dorph-Petersen, K. A., & Lewis, D. A. (2005). Mapping auditory core, lateral belt, and parabelt cortices in the human superior temporal gyrus. *The Journal of Comparative Neurology*, *491*(3), 270–289. https://doi.org/10.1002/cne.20702

Tadel, F., Baillet, S., Mosher, J. C., Pantazis, D., & Leahy, R. M. (2011). Brainstorm: A user-friendly application for MEG/EEG analysis. *Computational Intelligence and Neuroscience*, *2011*, 879716. https://doi.org/10.1155/2011/879716

Tobyne, S. M., Osher, D. E., Michalka, S. W., & Somers, D. C. (2017). Sensory-biased attention networks in human lateral frontal cortex revealed by intrinsic functional connectivity. *NeuroImage*, *162*, 362–372. https://doi.org/10.1016/j.neuroimage.2017.08.020

Uusitalo, M. A., & Ilmoniemi, R. J. (1997). Signal-space projection method for separating MEG or EEG into components. *Medical & Biological Engineering & Computing*, *35*(2), 135–140. https://doi.org/10.1007/BF02534144

Van Essen, D. C., Glasser, M. F., Dierker, D. L., Harwell, J., & Coalson, T. (2012). Parcellations and hemispheric asymmetries of human cerebral cortex analyzed on surface-based atlases. *Cerebral Cortex*, *22*(10), 2241–2262. https://doi.org/10.1093/cercor/bhr291

Woldorff, M. G., Gallen, C. C., Hampson, S. A., Hillyard, S. A., Pantev, C., Sobel, D., & Bloom, F. E. (1993). Modulation of early sensory processing in human auditory cortex during auditory selective attention. *Proceedings of the National Academy of Sciences of the United States of America*, *90*(18), 8722–8726.

Zatorre, R. J., Mondor, T. A., & Evans, A. C. (1999). Auditory attention to space and frequency activates similar cerebral systems. *NeuroImage*, *10*(5), 544–554. https://doi.org/10.1006/nimg.1999.0491

SUPPORTING INFORMATION

Additional supporting information can be found online in the Supporting Information section at the end of this article.

How to cite this article: Curtis, M. T., Ren, X., Coffman, B. A., & Salisbury, D. F. (2023). Attentional M100 gain modulation localizes to auditory sensory cortex and is deficient in first-episode psychosis. *Human Brain Mapping*, *44*(1), 218–228. https://doi.org/10.1002/hbm.26067